LABORATORY REPORT 5
Surface Brightness & Extragalatic Astronomy

Kirsten Howley [1]
Group 2 [2]
December 7, 2001

1. BACKGROUND & MOTIVATION

The Universe is filled with many enormous, immense objects, much of which amazingly can be studied by the tiny photons they emit. We commonly do this on clear nights when we gaze upon the many stars with our naked eye. Quite disappointingly though, these stars which twinkle in the night merely look like enlargements of the customary tiny dots when looked at through a telescope. With the nake eye though, galaxies are much more elusive. If you are patient, and have good periphirial vision, you might be able to spot the smudge of galaxy with the naked eye. However, imaging with a telescope provides spectacular results and detail, none of which would have ever been realized without the aid of optical devices.

Beyond the mere beauty of these magnificant objects, much information about or own Milky Way and the Universe can be derived from observation of these distant worlds. Techniques used in Labs 1-4 are all employed here: statistics, programming, imaging, analysis. The morphologies and brightness of galaxies can be constructed by combining the many tools that have been learned in Astro 122 Lab.

2. EQUIPMENT

The Leuschner 30-inch telescope, which operates on celestial coordinates was used to obtain infrared images. Taking images from the Leuschner telescope and infrared camera involved a remote login to the system 128.32.197. Once in the system, the dome needed to be opened and positioned to look out the slit, a filter need to be selected (the K filter, H filter, J filter, and aluminum plug were used for this lab), the flip mirror had to be opened, and the telescope had to be focused and pointed at the desired location. Since the Leuschner telescope operates on celestial coordinates, one needed to verify that the desired object was presently within viewing range (above the horizon) before imaging an object. Images were taken with selected exposure times using the *qimage* command. Files were exported from the remote system into the local system using *sftp*.

---

[1] E-mail: kirsten@ugastro.berkeley.edu

[2] Members: Friedman, A., Lau, L., Potapenko, J., Tai, C.

3. INTENSITY

Galaxies are extended objects, in contrast to stars which are point sources. Because of this, even if we were magically able to take away the affects of the smeared light of the galaxy, it would still be spread out over many pixels. For this reason, instead of measuring the total flux of a galaxy, the flux density, or intensity, is used. Intensity has units erg s^{-1} cm^{-2} sr^{-1}.

Since the measurement of the intensity of a galaxy includes units of steradians, it is necessary to know the conversion factor between the area of a pixel and a steradian. A steradian is a dimensionless unit that measures the angular area corresponding to a patch on a sphere; it is essentially 1 rad^2. There are 4π steradians in a sphere. Figure 1 demonstrates the solid angle the beam sweeps out and the corresponding 'patch' of area on the sphere.

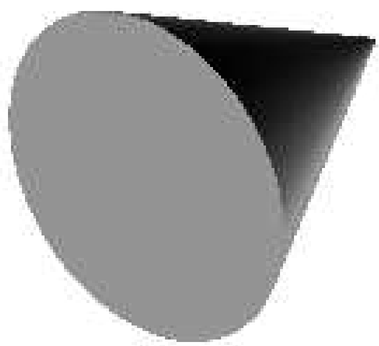

Fig. 1.— Cone represents the "flashlight" effect of a steradian sweeping out an angular area, and corresponding to a surface area on a sphere.

Converting pixels to steradians is a relatively simple procedure. First, converting pixels into square degrees:

$$1\,pixel \times \frac{(1.35'')^2}{pixel} \times \left(\frac{1'}{60''}\right)^2 \times \left(\frac{1^\circ}{60'}\right)^2 = 1.406 \times 10^{-7} deg^2$$

then converting steradians into square degrees:

$$1\,sr = 1\,rad^2 \times \left(\frac{360^\circ}{2\pi}\right)^2 = 3,283\,deg^2$$

dividing a pixel by a steradian yields:

$$1\,pixel = 4.284 \times 10^{-11}\,sr$$

4. SKY BRIGHTNESS

Signal to noise is important when imaging objects, especially in the near-infrared, which is where our planet and atmosphere emit heavily. If there were no noise, it would be ideal to image galaxies in the K-band, where extinction would be minimal.

In order to determine the best band to image galaxies in, the sky brightness needed to be quantified. Data from Lab 4 was used to measure the level of the sky background in J, H & K bands. In each band, 27 dithered images were taken of a part of the sky relatively devoid of stars. Each image was dark subtracted and flatfielded. The median counts per pixel for each image was then multiplied by gain and converted into units of flux per steradian. The intensity of the sky was calculated using standard stars as a correlation between flux and magnitude. The sky level for each band is plotted in Figure 2. Note that the plot variation of the sky pictures is much less than possion variations, negating the need for a mosaic of sky level images to determine the sky level background.

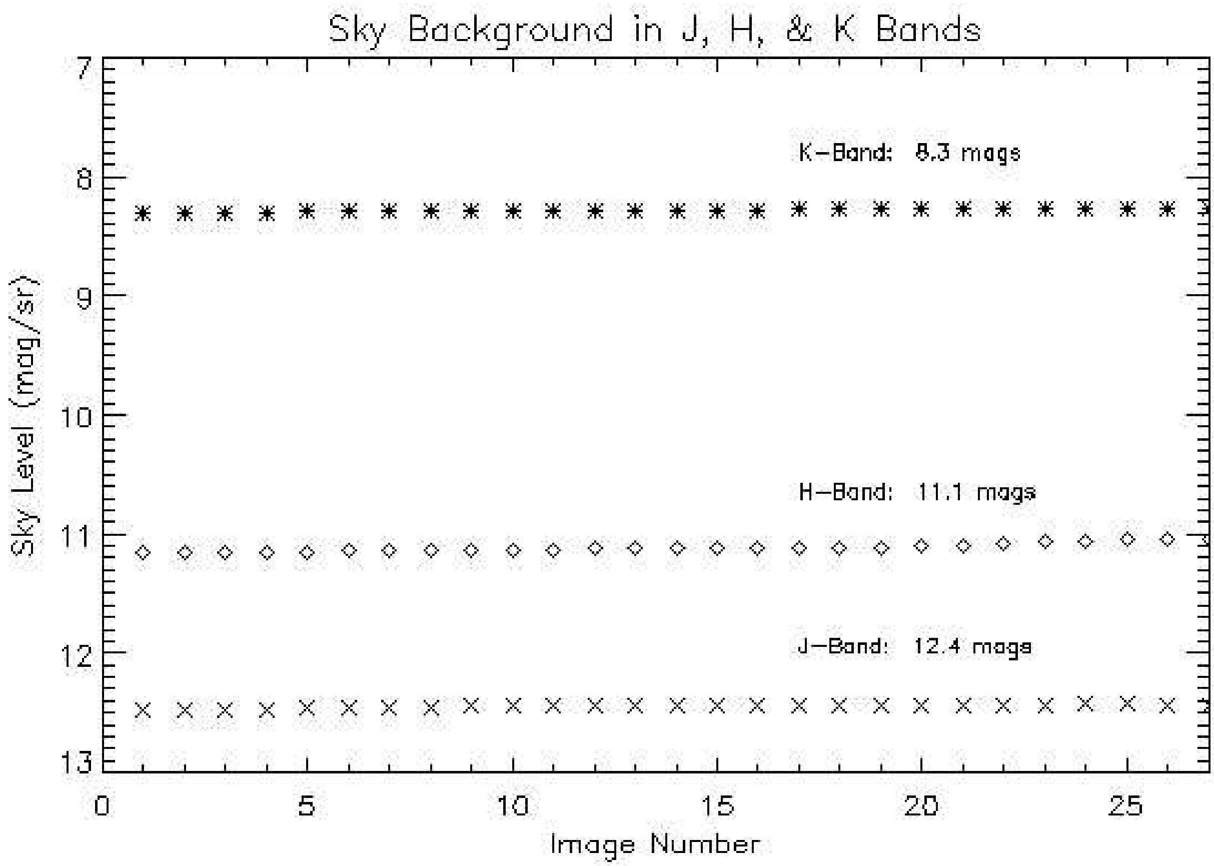

Fig. 2.— Sky level in J, H & K bands. 27 separate images in each band was taken of a portion of sky relatively devoid of stars and plotted to determine the sky brightness.

The magnitudes can be converted into cgs units using the known flux of Vega in the three bands:

$$F_\nu = 10^{-0.4\,m_\nu} \cdot F_{\nu_{Vega}}$$

and conversion from mks to cgs units:

$$\frac{W \cdot s \cdot 10^3}{m^{-2} \cdot sr} \Rightarrow \frac{erg}{s \cdot cm^2 \cdot sr}$$

The intensity in magnitudes per steradian and in erg s^{-1} cm^{-2} sr^{-1} is displayed in Table 1.

Table 1: Intensity of sky in J, H, & K bands in magnitudes per steradian and in cgs units.

Band	Wavelength (nm)	Intensity (magnitudes/sr)	Intenstity ($ergs^{-1}$ cm^{-2} sr^{-1})
J	1220	12.4	9.4
H	1630	11.1	20.3
K	2190	12.4	167.0

The K-band would be the ideal wavelength to image galaxies in based on the KIII star like properties galaxies exhibit. That is, galaxies tend to peak at the same wavelength as K stars, which is around the L band. Since the K band is the closest to L of the three bands, we would expect a relatively higher flux in that wavelength. Unfortunately, our atmosphere counteracts this benefit. Figure 2 clearly demonstrates our atmosphere's brightness in K. Based on properties of our atmosphere, the J band would be the ideal wavelength to image in. It turns out that the combination of atmospheric and galactic properties results in the H band being the best wavelength to image in.

In order to increase our signal to noise ratio, we must increase our effective exposure time. Doing this will allow us to detect fainter and fainter signals. We can increase exposure time by increasing the time we image an object, however, as we saw in Lab 4, saturation can occur relatively quickly. The alternative is to increase the number of exposures. We can decrease our signal to noise ratio by $\sqrt{N}$, from Poisson statistics. In this lab, we imaged each of our galaxies 50 times, thus increasing our signal to noise ratio by as much as a factor of 7 in some areas.

5. GALAXY PHOTOMETRY

5.1. M 105

M105 is an elliptical galaxy located 13,676 kpc away, at RA 10:47 DEC +12:34[3]. A mosaic was created in the H-band using 50 rastered images; a reverse color portion of the mosaic containing M 105 is displayed in Figure 3. The galaxy was contoured using a logarithmic scale. The low value was taken as an average of one standard deviation of the counts per pixel for the various images (approximately 0.6 counts). This was done to keep isophotes consistent from image to image[4]. The upper value was set to be greater than the maximum counts per pixel of the image, since isophotes would be unaffected at values above the maximum. The increment between each individual isophote is $10^{0.2}$ counts. This increment was used so that detail could be observed. The contour plot is displayed in Figure 3.

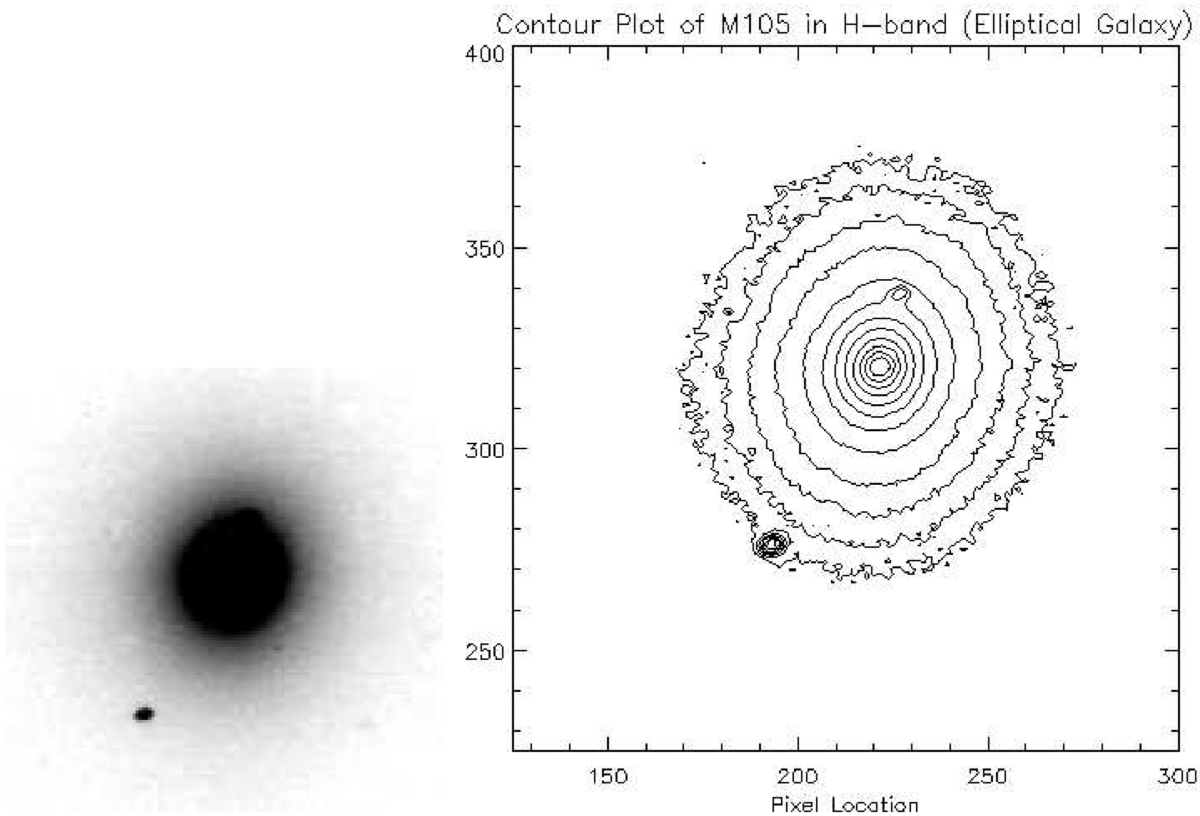

Fig. 3.— M 105 in H-band & Contour Plot. Isophotes are on a logarithmic scale in increments of $10^{0.2}$ counts. Note that the isophotes are coaxial.

---

[3]Information obtained from http://simbad.u-strasbg.fr/simbad

[4]With the exception of NGC 891 whose noise made it necessary to start at 2.5 standard deviations.

Observation of the contour plot reveals symmetrical distribution of counts about the center of the galaxy. An occasional star produces an unexpected spot, but otherwise the counts fall off relatively quickly and uniformly from the center.

5.2. M 95

M 95 is a face-on SBb barred spiral galaxy located 11,969 kpc away, at RA 10:43 DEC +11:42[5]. A mosaic was created of the galaxy in the H-band using 50 rastered images. The galaxy in reverse color and a contour plot is displayed in Figure 4.

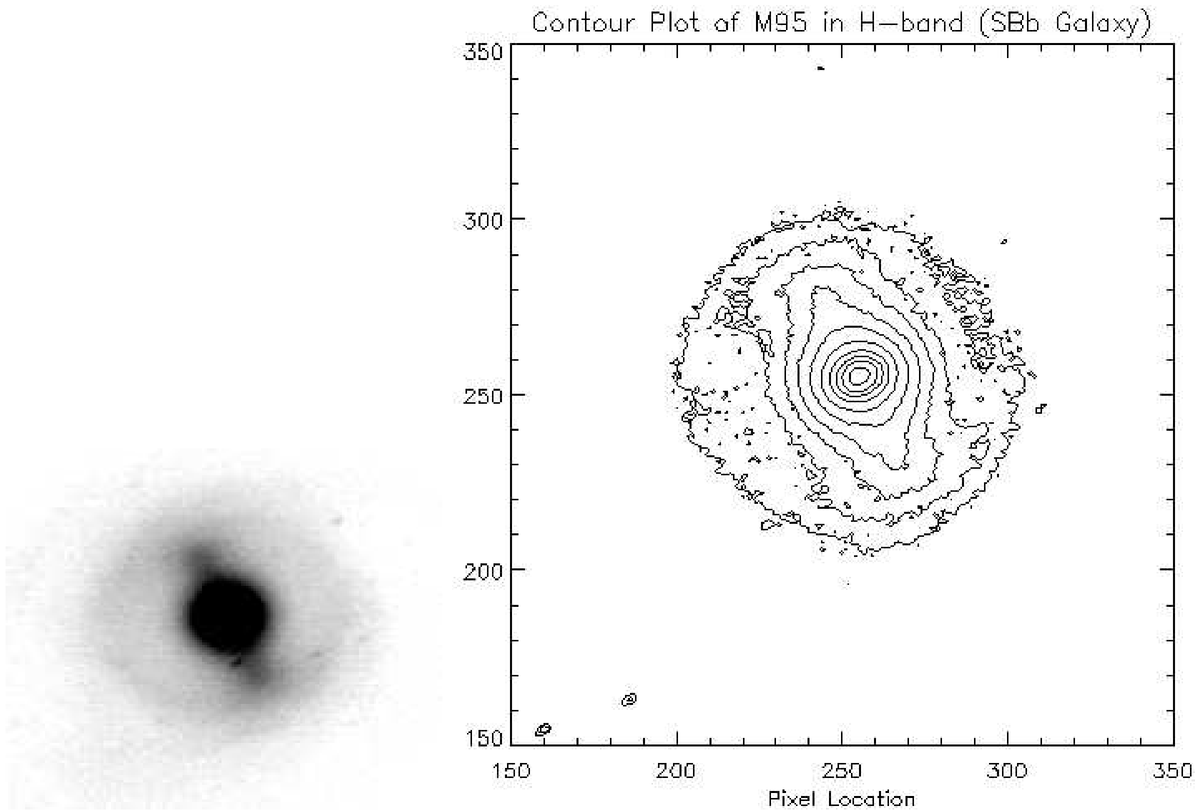

Fig. 4.— M 95 in H-band & Contour Plot. Isophotes are on a logarithmic scale in increments of $10^{0.2}$ counts. Note the distinct bars of the galaxy in the contour plot.

Observation of the contour plot reveals distinct bars in the barred spiral and a diffuse distribution of the spirals encompassing the galaxy. Even the direction of each spiral is apparant in the contour plot, which was not as obvious in the image.

[5]Information obtained from http://simbad.u-strasbg.fr/simbad

5.3. NGC 1637

NGC 1637 is a face-on bright SAb galaxy; it is a hybrid between a barred spiral and a regular spiral[6]. It is located 11,030 kpc away, at RA 04:41 DEC -02:51[7]. A mosaic was created of the galaxy in the H-band using 50 rastered images. The galaxy in reverse color and a contour plot is displayed in Figure 5.

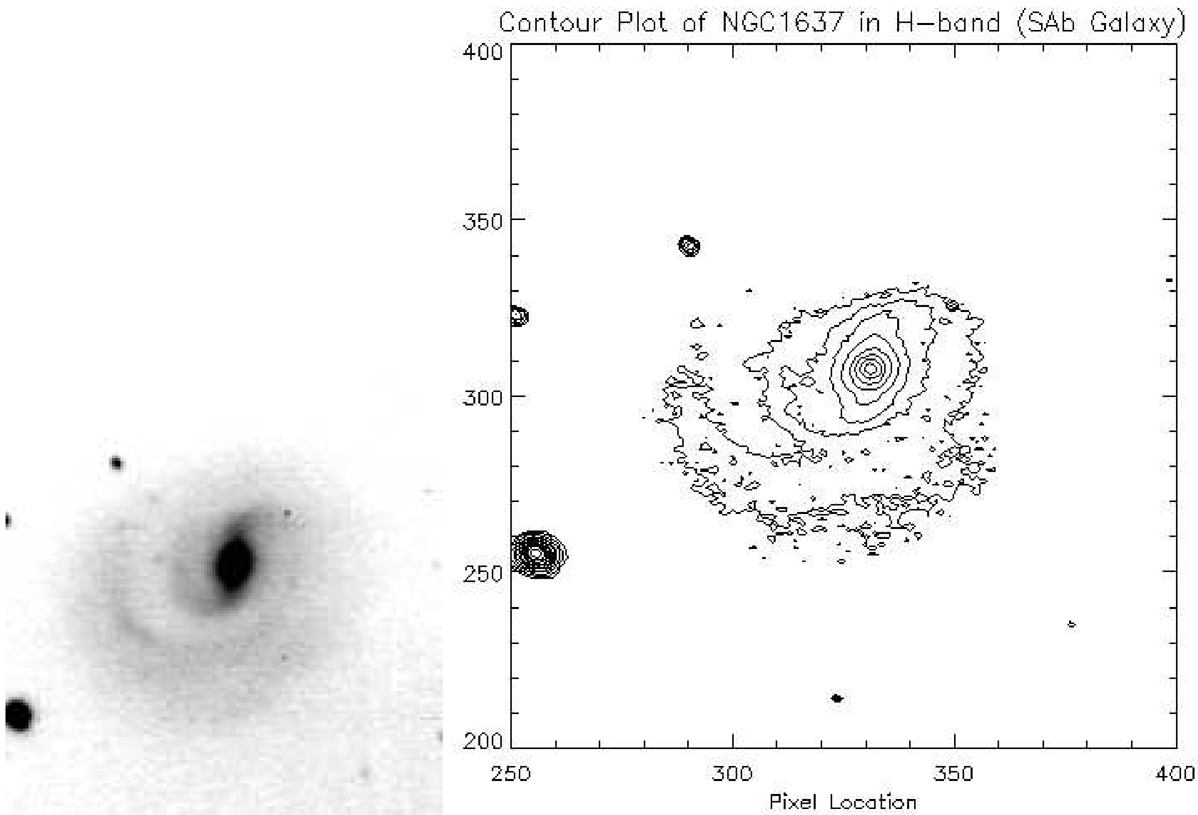

Fig. 5.— NGC 1637 in H-band & Contour Plot. Isophotes are on a logarithmic scale in increments of $10^{0.2}$ counts. Note the strong spiral arm on the underside of the galaxy (the distortion is likely due to the collision with another galaxy) and the distinct bars of the galaxy in the contour plot.

Observation of the contour plot reveals a single distinct arm. The distortion suggests some sort of gravitational interaction with another galaxy. Also, distinct bars are seen in the plot in a S-shaped structure.

---

[6]Information on galaxy structure obtain from: http://members/tripod.com/∼btboar/Galaxies.html

[7]Information obtained from http://simbad.u-strasbg.fr/simbad

5.4. NGC 891

NGC 891 is an edge-on SBb spiral galaxy located 8,123 kpc away at RA 02:22 DEC +42:20[8]. A mosaic was created of the galaxy in the H-band using 50 rastered images. The galaxy in reverse color and a contour plot is displayed in Figure 6.

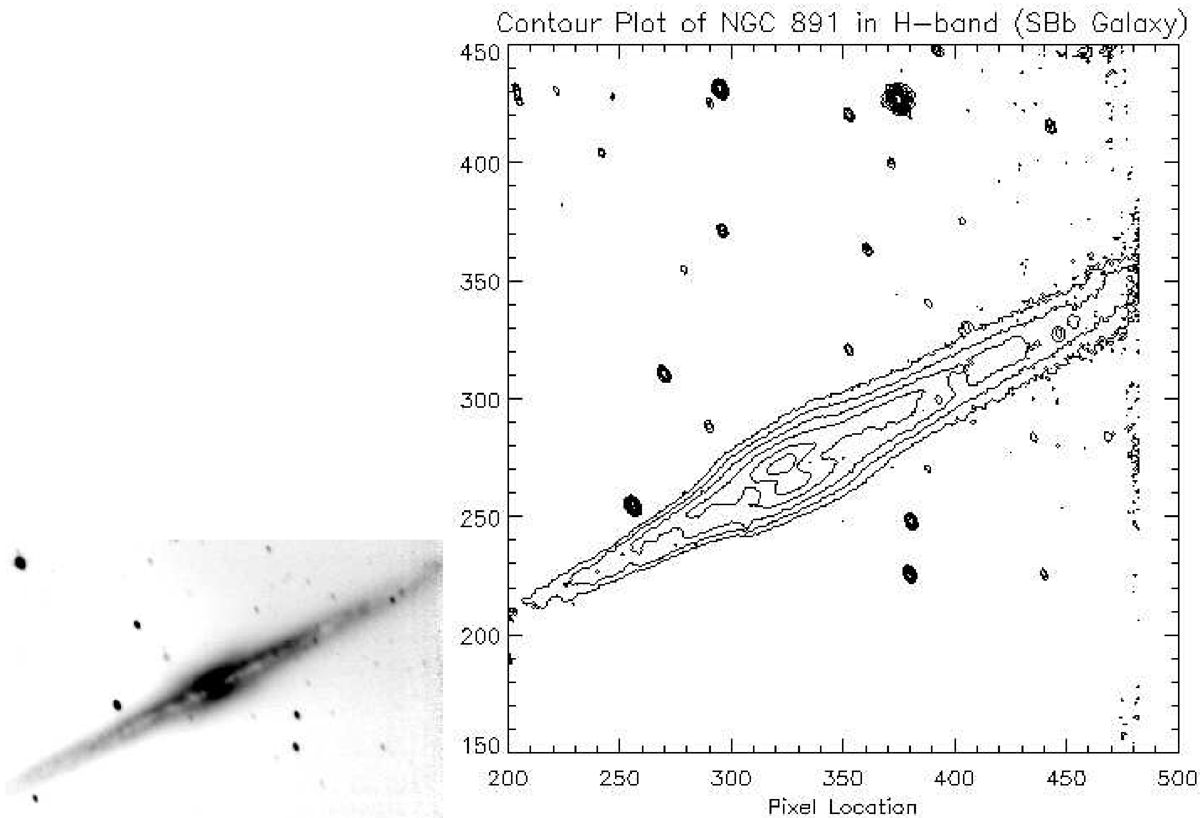

Fig. 6.— NGC 891

Observation of the contour plot reveals a significant amount of extinction. This would be expected since the galaxy is edge on. In a face-on spiral galaxy, less light is extincted since the large surface area permits the majority of light generated by the galaxy to be transmitted in our direction. However, in the edge on spiral, the surface area is significantly smaller. Dust within the plane of the galaxy extincts much of the light. The contour plot demonstrates this by showing strong, sharp intrusion into the center of the galaxy.

The extinction of NGC 891 can be furthered studied by imaging the galaxy in the J, H, and K bands. Images were taken in all three bands, transformed into mosaics, and aligned. A sample of 16 pixels was taken from the bulge in each of the three mosaic images in order to represent an

[8]Information obtained from http://simbad.u-strasbg.fr/simbad

unextincted portion of the galaxy. Another sample of 298 pixels was taken from the extincted edge. The intensity for each pixel was then computed in the J, H, and K bands. The H-K magnitudes were plotted against the J-H magnitudes for both the extincted and unextincted portions of the galaxy. Figure 7 displays all these points.

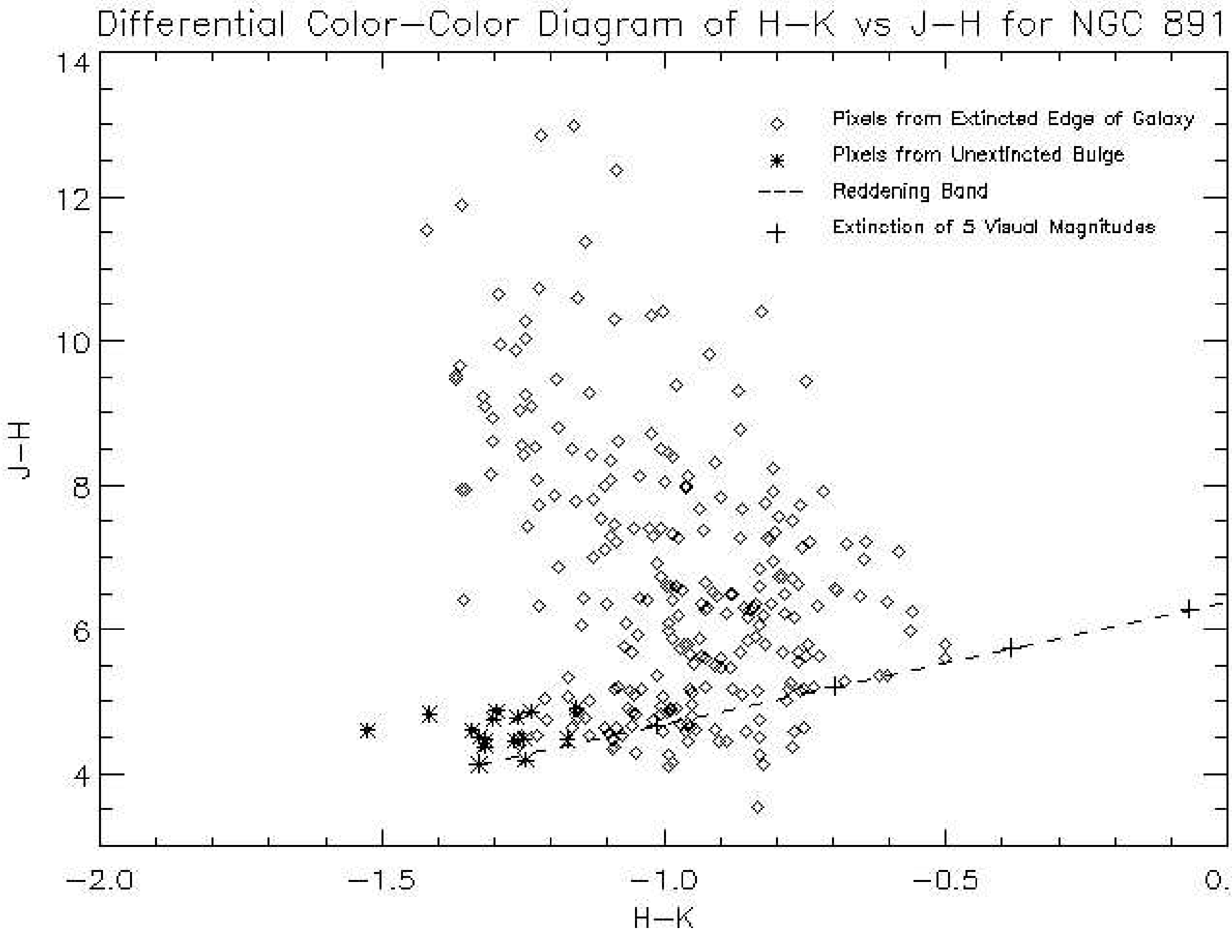

Fig. 7.— Color-Color diagram for the extinction along the edge of NGC 891.

In Figure 7, the wide scatter of points makes it difficult to determine the extinction along the edge of NGC 891. In order to be able to make a determination of the average extinction, the median value of H-K and J-H was calculated for both the unextincted bulge and extincted edge. These two points were plotted and the error computed by taking the standard deviation. Although each point was an individual sample, it cannot be assumed that the mean value of each point corresponds to some 'true' mean value. That is, it would be expected that extinction would vary over the edge of the galaxy; areas closer to the galactic plane would experience more extinction than areas further away. For this reason, the standard deviation of points was used as opposed to the standard deviation of the mean. The results are plotted in Figure 8.

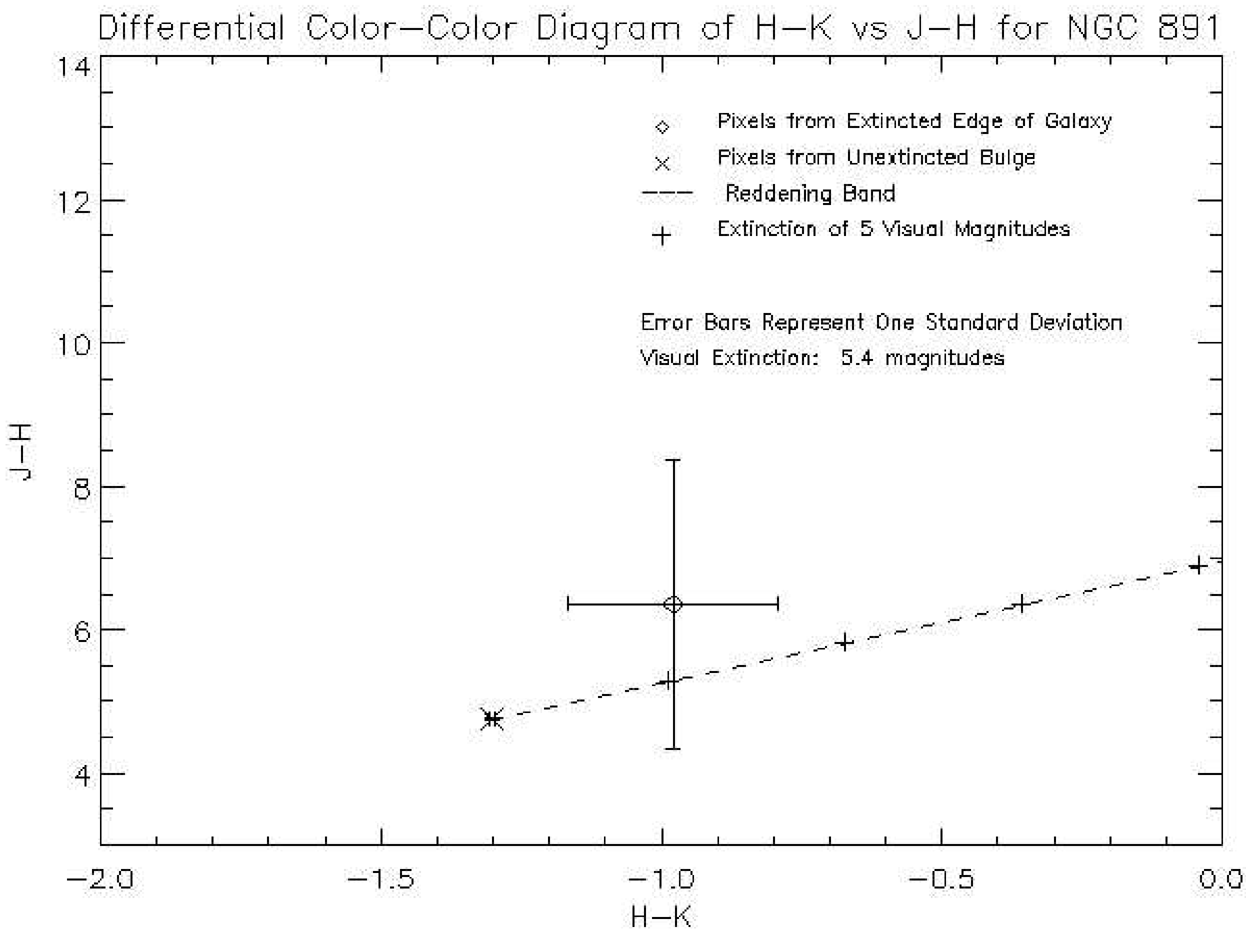

Fig. 8.— Averaged Color-Color diagram for the extinction along the edge of NGC 891.

The averaged H-K, J-H extincted point was regressed down to the unextincted point to determine the average extinction in the visual band. Table 2 lists the average extinction in each band using A/A_ν values from Lab 4.

Table 2: Average extinction in J, H, & K bands along edge of NGC 891.

Band	Wavelength (nm)	A (mags)
V	551	5.4
J	1220	1.5
H	1630	0.9
K	2190	0.6

A tri-color image of NGC 891 can be found at www.ugastro.berkeley.edu/~kirsten/.

5.5. Intensity

To determine a relationship between radius and intensity, four separate galaxies were imaged: NGC 1637 (SAb galaxy), M 95 (SBb galaxy), M 105 (Elliptical galaxy), and NGC 2775 (S0 galaxy). A reverse color H-band image of NGC 2775 is displayed in Figure 9.

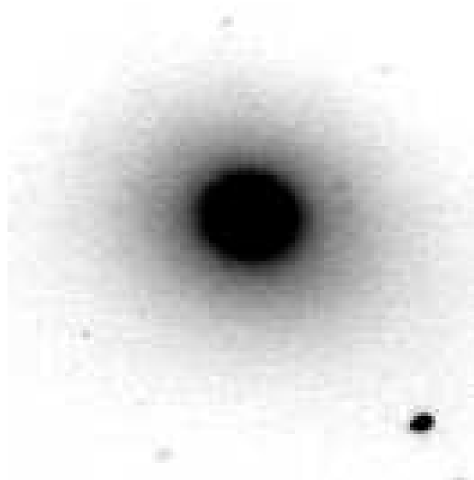

Fig. 9.— NGC 2775 in the H-Band (S0 galaxy).

In order to find the correlation between surface brightness of a galaxy and the distance from the center, the brightest point in each galaxy was found by convolving the mosaic image. Since the center would be the most luminous, using the brightest point of each galaxy ensured that we would locate the center[9]. The intensity of each pixel was measured and the corresponding distance from the center pixel noted. In order to determine the true distance from the center, the physical length of each pixel had to be calculated.

The angular extent of each galaxy was converted into a physical length using the distance to the galaxy, Hubble's law, and the ression velocity[10]:

$$d = \frac{v}{H_0}$$

Using a value for Hubble's constant of 65 km s^{-1} Mpc^{-1} the distances to galaxies could easily be computed[11]. The small angle approximation was used to determine the distance a pixel represented for each galaxy:

$$sin(\theta) = \theta$$

[9]Unless, of course, there was a star in our line of sight.

[10]Recession velocity obtained from http://nedwww.ipac.caltech.edu/

[11]Carroll, Bradley W., Dale Ostlie, A.

The physical length, s, of a pixel could then be determined by:

$$s = \theta d$$

Table 3 lists the recession velocity, distance to galaxy, and the physical length of a pixel for each galaxy:

Table 3: Recession Velocity, Distance and Pixel Length for Spiral & Elliptical Galaxies

Galaxy	Type	Recession Velocity	Distance to Galaxy	Length of a Pixel
		km/s	Mpc	kpc
NGC 1637	SAb	717	11.0	0.07
M 95	SBb	778	12.0	0.08
M 105	E	911	14.0	0.09
NGC 2775	SO	1354	20.8	0.14

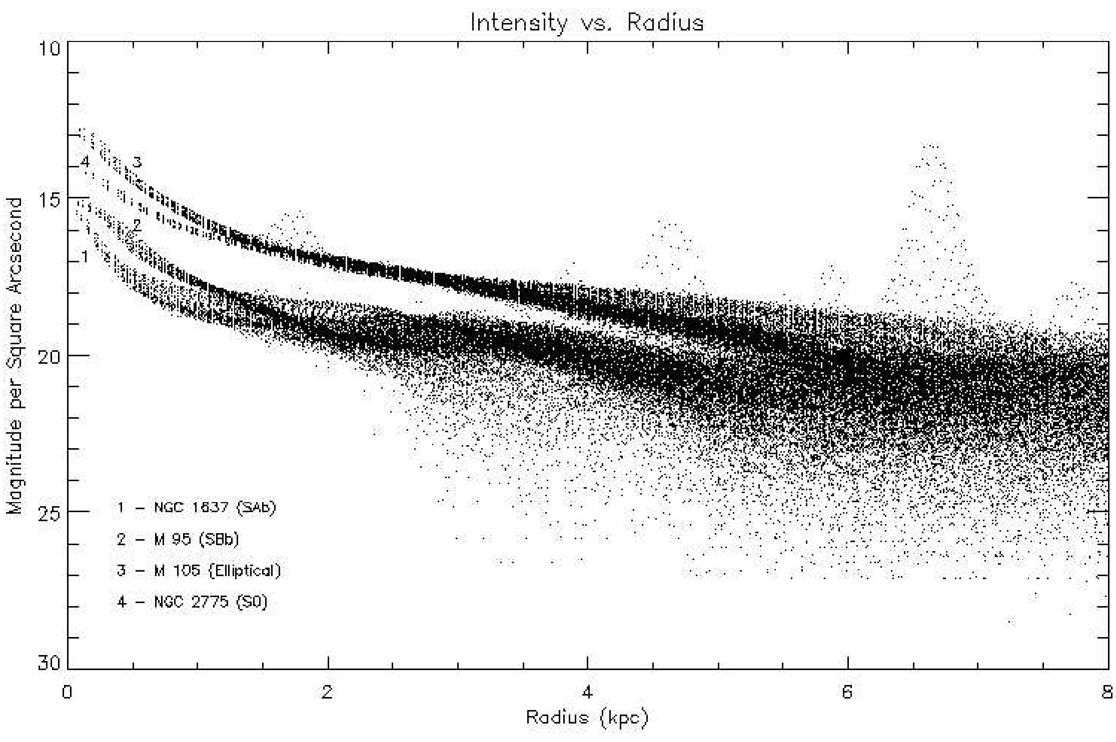

Fig. 10.— Intensity vs Radius for NGC 1637, M 95, M 105 and NGC 2775 (an S0 galaxy).

The corresponding distance from the center and intensity for each of the four galaxies is plotted in Figure 10.

An important known relationship for elliptical galaxies and the bulges of spirals is Vaucoulerurs Law, which relates intensity to radius:

$$I(R) = I_e \times e^{-7.67((R/R_e)^{\frac{1}{4}}-1)}$$

where R_e is the radius at which one half of the total flux from the galaxy falls, and I_e is the intensity at that radius.

Another important relation for the disks of spiral galaxies is Freeman's Law, which equates intensity to radius beyond the bulge:

$$I(R) = I_0 \times e^{-R/h_R}$$

where h_R is the length at which the intensity has decreased by a factor of e: I_0/e.

In order to see if either of these relationships exists, the average intensity per radius was plotted in Figure 11.

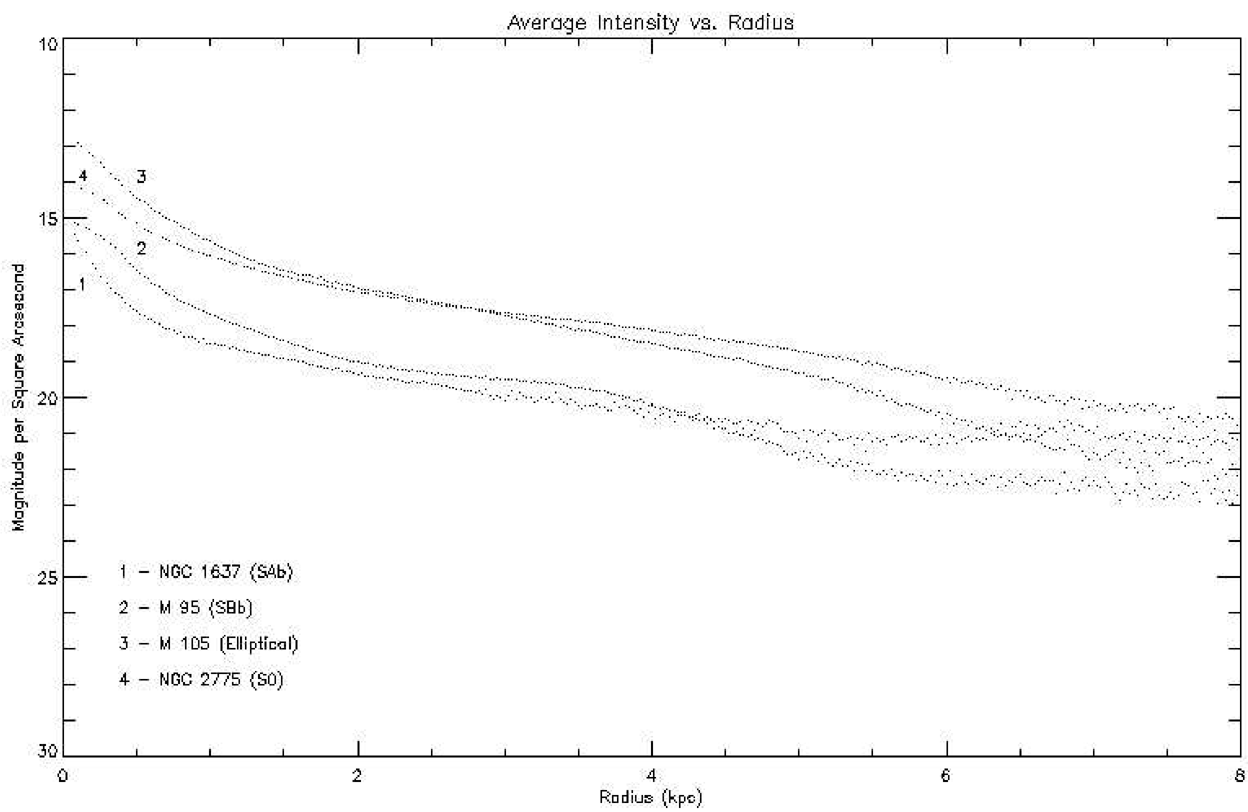

Fig. 11.— Average Intensity vs Radius for NGC 1637, M 95, M 105 and NGC 2775. Intensity values were averaged over radius in increments of .01 kpc.

To get a closer look at the structure of a galaxy and its intensity as it pertains to Vaucoulerurs Law and Freeman's Law, a zoom in was done on NGC 1637, and both laws overplotted to see if there was a correlation. Figure 12 demonstrates a strong fit for both the bulge part of the spiral galaxy as well as the disk component.

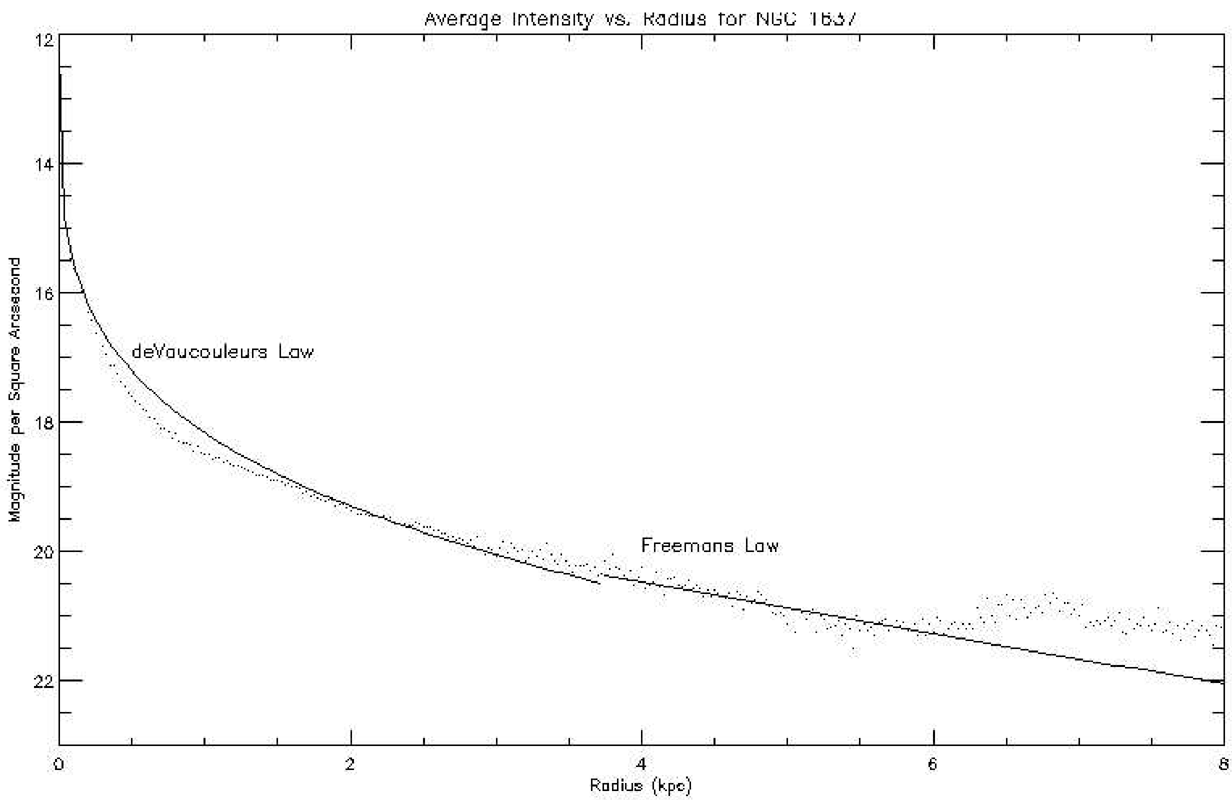

Fig. 12.— Intensity vs Radius for NGC 1637 and an overplot of Freeman's Law and deVaucoulers Law. Note the close fit.

6. CONCLUSIONS

Amazingly, these distant objects, far from eachother, with only the ability to communicate by tiny wave packets have managed to evolve into enormous objects which all closely obey all the same laws. It is true that their structure may vary slightly, but of the thousands of objects cataloged, most fall into the few categories developed. How is that possible? Truly this amazing organization shows the power of physics. Studying other galaxies provides insight into our own and provides a few answers about our development and structure. I think more importantly though, studying distant galaxies produces more questions and pondering about our vast universe.

This lab allowed us to observe a range of galaxy types and understand how and why they are different. Also, studying the variation of intensity over these extended objects allows us to postulate about the internal structure and composition of some of these galaxies. Of course, as mentioned before, discovery often leads to more questions, and one could easily spend an entire lifetime studying the structure of these gorgeous creations.

7. ACKNOWLEDGEMENTS

Since this is my last, and final lab (whimper) I would like to express my great appreciation to both Professor Graham and Nate McCrady. I have to say, without a doubt, this is the most fulfulling class I have ever taken. Yes, sometimes I may have completed my lab kicking & screaming, but in the end, it was always well worth the effort. I have to say, even if I go on and decide not to do astronomy, but rather open a bar in Baja and hang my astrophysics degree on the wall alongside my liquor license, I will always be grateful for this class, for this has been an experience I will never forget. I'm actually quite sad that its over. Yawwwwwnnn! Okay, time to sleep!

8. REFERENCES

Carroll, Bradley W., Dale Ostlie, A. *An Introduction to Modern Astrophysics.* Addison-Wesley Publishing Co., 1996.

McCrady, Nate. *Lab 5*

Taylor, John R. *An Introduction to Error Analysis.* Sausalito: University Science Books, 1997.